

# Lattice QCD thermodynamics with Wilson quarks

Shinji EJIRI<sup>\*)</sup>

*Physics Department, Brookhaven National Laboratory,  
Upton, New York 11973, USA*

We review studies of QCD thermodynamics by lattice QCD simulations with dynamical Wilson quarks. After explaining the basic properties of QCD with Wilson quarks at finite temperature including the phase structure and the scaling properties around the chiral phase transition, we discuss the critical temperature, the equation of state and heavy-quark free energies.

## §1. Introduction

In order to remove theoretical uncertainties in the analysis of data from heavy-ion collision experiments, first principle calculations by the lattice QCD are indispensable and various interesting results have been already reported. However, most lattice QCD studies at finite temperature ( $T$ ) and chemical potential ( $\mu_q$ ) have been performed using staggered-type quark actions with the fourth-root trick of the quark determinant so far. Therefore, studies by the other actions such as Wilson-type quark actions are necessary to estimate systematic errors due to lattice discretization.

In this report, we want to highlight the QCD thermodynamics by numerical simulations with dynamical Wilson quarks. A systematic study of the QCD thermodynamics has been done by the CP-PACS Collaboration using the Iwasaki (RG) improved gauge action and the 2 flavor clover improved Wilson quark action several years ago.<sup>1),2)</sup> Recently the WHOT-QCD Collaboration restarted the study by the same action adopting new technical developments.<sup>3)-5)</sup> In this review, we first explain in Sec. 2 the phase structure of 2 flavor QCD with Wilson quarks in the simulation parameter plane ( $\beta, K$ ). Then, the universality class of the chiral phase transition is discussed in Sec. 3. An estimation of the critical temperature in the chiral limit is given in Sec. 4. The equation of state (EoS) is discussed in Sec. 5, highlighting fluctuations at finite density, related to the physics of the possible critical point in the ( $T, \mu_q$ ) plane., and also results of heavy-quark free energies are shown in Sec. 6.

## §2. Phase structure of QCD with Wilson quarks

The lattice QCD with Wilson-type quarks is known to have a complicated phase structure due to the explicit violation of chiral symmetry and due to the existence of the parity-flavor broken phase (Aoki phase).<sup>6)</sup> Therefore, a systematic study surveying a wide range of the parameter space is required to determine appropriate simulation parameters. Moreover, lattice artifacts are large on coarse lattices used in

---

<sup>\*)</sup> e-mail address: ejiri@quark.phy.bnl.gov

most finite temperature simulations when the standard plaquette gauge action and the standard Wilson quark action are used, For example, unexpected strong phase transition is observed at intermediate quark masses in 2 flavor QCD. Therefore, we have to improve the lattice action to reduce these lattice artifacts.

Figure 1 (left) is the phase diagram obtained by the CP-PACS Collaboration for 2 flavor QCD with the RG-improved gauge action combined with the clover-improved Wilson quark action.<sup>1)</sup> The 2 flavor lattice QCD has two simulation parameters  $K$  and  $\beta$ .  $K$  is the hopping parameter in the quark action and  $\beta$  is  $6/g^2$  in the gauge action. The solid line  $K_c(T = 0)$  is the location of the chiral limit. The pion mass decreases as  $K$  increases from small  $K$ , and vanishes on the line  $K_c(T = 0)$  at zero temperature. In the region above  $K_c(T = 0)$ , a parity-flavor symmetry of the Wilson-type quark action is broken spontaneously.<sup>6)</sup> At zero temperature, the boundary of the parity-flavor broken phase is known to form a sharp cusp touching the free massless fermion point  $K = 1/8$  at  $\beta = \infty$ . However, the region above  $K_c(T = 0)$  is an unphysical parameter space, and we usually perform simulations below  $K_c$ . The region below  $K_c(T = 0)$  corresponds to the physical QCD with  $1/K - 1/K_c$  being proportional to the quark mass  $m_q$ .

At finite temperature, the parity-flavor broken phase retracts from the large  $\beta$  region. The colored region with the boundary  $K_c(T > 0)$  in Fig. 1 (left) is the parity-flavor broken phase at finite temperature for the temporal lattice size  $N_t = 4$ . When  $N_t$  is fixed, the temperature  $T = (N_t a)^{-1}$  becomes higher as  $\beta$  is increased, since the lattice spacing  $a$  becomes smaller. The dashed line  $K_t$  is the pseudo-critical line separating the hot and cold phases for  $N_t = 4$ . The region to the right of  $K_t$  (larger  $\beta$ ) is the high temperature quark-gluon plasma (QGP) phase, and that to the left (smaller  $\beta$ ) is the low temperature hadron phase. The crossing point of the  $K_c(T = 0)$  and the  $K_t$  is the chiral phase transition point.

As shown in this figure, the line that the pion mass vanishes at  $T > 0$  ( $K_c(T > 0)$ ) runs along the line of the chiral limit in the low temperature phase, while the  $K_c(T > 0)$  line bends sharply at the chiral phase transition point and goes to the unphysical region above  $K_c(T = 0)$ . This is consistent with the picture that the massless pion, i.e. the Goldstone boson associated with spontaneous chiral symmetry breaking, appears only in the cold phase.

### §3. O(4) scaling relation

Next, we discuss the natures of the chiral phase transition in the critical region. The order of the phase transition is expected to be second order for 2 flavor QCD and first order for 3 flavor QCD in the chiral limit. The confirmation of this expectation is an important step toward the clarification of the QCD transition in the real world. In this section, we discuss the scaling behavior of 2 flavor QCD.

When the chiral transition of 2 flavor QCD is second order, the transition is expected to be in the same universal class with a 3-dimensional O(4) spin model. With the identifications  $M \sim \langle \bar{\Psi}\Psi \rangle$  for the magnetization,  $h \sim m_q a$  for the external magnetic field and  $t \sim \beta - \beta_{ct}$  for the reduced temperature, where  $\beta_{ct}$  is the chiral transition point, we expect the same scaling behavior as the O(4) spin model.

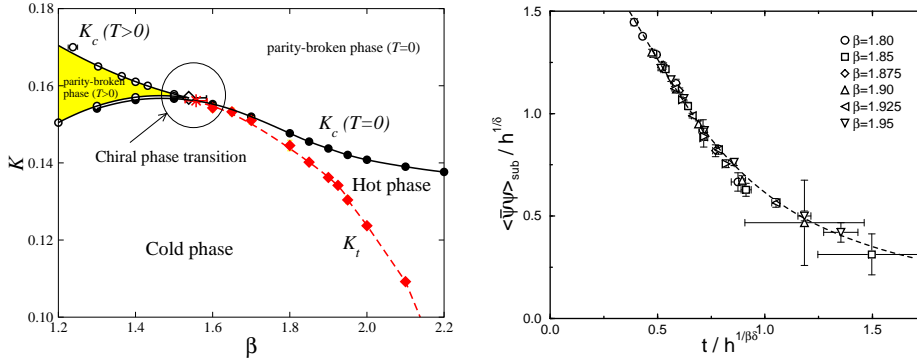


Fig. 1. Left: Phase diagram for the RG-improved gauge and clover-improved Wilson quark actions on an  $Nt = 4$  lattice. Right:  $O(4)$  scaling relation of the chiral condensate.<sup>1)</sup>

The  $O(4)$  scaling was first tested with staggered fermion by Karsch and Laermann.<sup>7)</sup> The study was extended to a wider range of the quark mass and lattice sizes by several groups.<sup>8)–11)</sup> However, an agreement of the critical exponents between the  $O(4)$  spin model and QCD with 2 flavors of staggered quarks has not been obtained.

For the case of Wilson quarks, Iwasaki et al.<sup>12)</sup> investigated the scaling relation,

$$M/h^{1/\delta} = f(t/h^{1/\beta\delta}), \quad (3.1)$$

using the standard Wilson quark action coupled to RG-improved gluon. They identified the subtracted chiral condensate defined by an axial Ward-Takahashi identity,<sup>13)</sup>  $\langle \bar{\Psi}\Psi \rangle_{\text{sub}} = 2m_q a Z \sum_x \langle \pi(x)\pi(0) \rangle$ , as the magnetization of the spin model. Here, the quark mass  $m_q$  is defined by an axial vector Ward-Takahashi identity,<sup>13)</sup>  $m_q^{\text{AWI}}$ , and the tree-level renormalization coefficient  $Z = (2K)^2$  was adopted. They found that the scaling relation Eq. (3.1) is well satisfied with the critical exponents and the scaling function of the  $O(4)$  spin model.

The  $O(4)$  scaling has been obtained also with improved Wilson quarks. Figure 1 (right) is the result for the case of the clover-improved Wilson quark action coupled with the RG gauge action, obtained on a  $16^3 \times 4$  lattice.<sup>1)</sup> The vertical axis is  $M/h^{1/\delta}$  and the horizontal axis is  $t/h^{1/\beta\delta}$ , where  $\beta$  and  $\delta$  are the critical exponents obtained in the  $O(4)$  spin model. The dashed line is the  $O(4)$  scaling function. They fitted the data to the scaling function adjusting  $\beta_{ct}$  and the scales of two axes. As seen from Fig. 1 (right), QCD data is well described by the  $O(4)$  scaling ansatz. This result suggests that the chiral phase transition is of second order for 2 flavor QCD.

#### §4. Critical temperature of 2 flavor QCD

The critical temperature ( $T_c$ ) is one of the most fundamental quantities in the QCD thermodynamics and is important in phenomenological studies of heavy ion collisions. Recently several groups<sup>14)–16)</sup> have tried to determine  $T_c$  near the physical mass parameter in 2+1 flavor QCD by simulations with improved staggered quarks. However, the results are still contradictory to each other.

The WHOT-QCD Collaboration reported recently a preliminary result of  $T_c$  for

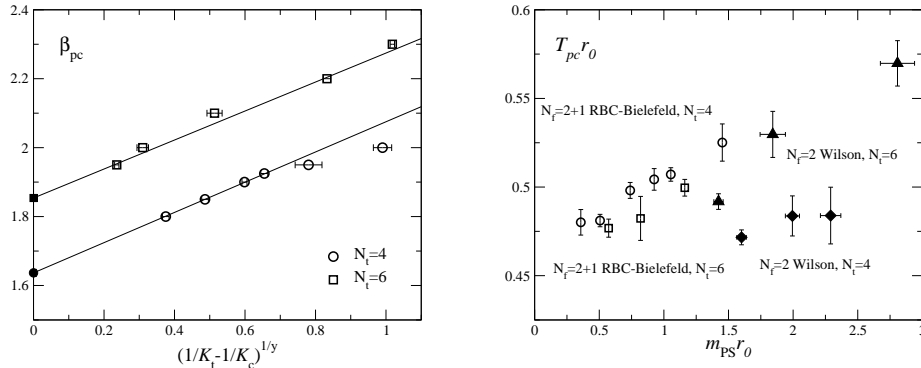


Fig. 2. Left: The pseudo-critical point  $\beta_{pc}$  as a function of  $m_q \sim 1/K - 1/K_c$  for  $N_t = 4$  (circle) and  $N_t = 6$  (square).<sup>4)</sup> Right: Comparison of  $T_{pc}$  scaled by  $r_0$  between the staggered quark action (open symbol)<sup>15)</sup> and the Wilson quark action (filled symbol)<sup>4)</sup> for  $N_t = 4$  and 6.

2 flavor QCD renewing the analysis done in Ref. 1).<sup>4)</sup> They determined the pseudo-critical points  $\beta_{pc}$  defined from the peak of the Polyakov loop susceptibility on  $16^3 \times 4$  and  $16^3 \times 6$  lattices, as a function of the hopping parameter  $K$ .

As seen in the previous section, the subtracted chiral condensate satisfies the scaling behavior with the critical exponents and scaling function of the 3-dimensional O(4) spin model. Assuming that the pseudo-critical temperature from the Polyakov loop susceptibility follows the same scaling law as the O(4) spin model, i.e.  $t_{pc} \sim h^y$  with  $y \equiv \beta\delta = 0.537(7)$ , the data of  $\beta_{pc}$  in Fig. 2 (left) are fitted by  $\beta_{pc} = \beta_{ct} + Ah^{1/y}$  with two free parameters,  $\beta_{ct}$  and  $A$ , in the range of  $\beta = 1.8$ – $1.95$  for  $N_t = 4$  and  $\beta = 1.95$ – $2.10$  for  $N_t = 6$ . First, they adopted the definition  $m_q a \sim 1/K - 1/K_c$  as the quark mass where  $K_c$  is the chiral point where the pion mass vanishes at  $T = 0$  for each  $\beta$ . The critical temperature  $T_c$  is calculated in the chiral limit using  $T = 1/(N_t a)$ . The lattice spacing  $a$  is estimated from the vector meson mass assuming  $m_V(T = 0) = m_\rho = 770$  MeV at  $\beta_{ct}$  on  $K_c$ . By this procedure, They obtained preliminary results of  $T_c = 183(3)$  MeV for  $N_t = 4$  and  $174(5)$  MeV for  $N_t = 6$ . They also calculated  $\beta_{ct}$  using the relation of  $m_q^{\text{AWI}} \propto m_{PS}^2$ , where  $m_{PS}$  is the pseudo-scalar meson mass and  $m_q^{\text{AWI}}$  is the quark mass obtained from the axial vector Ward-Takahashi identity. The results of  $T_c$  are  $173(3)$  MeV ( $N_t = 4$ ),  $167(3)$  MeV ( $N_t = 6$ ) for  $h = (m_{PS} a)^2$  and  $176(3)$  MeV ( $N_t = 4$ ) for  $h = m_q^{\text{AWI}} a$ . It is noted that these O(4) fits reproduce the data of  $\beta_{pc}$  much better than a linear fit  $\beta_{pc} = \beta_{ct} + Ah$ . A tentatively conclusion is that the critical temperature in the chiral limit is in the range 170–186 MeV for  $N_t = 4$  and 164–179 MeV for  $N_t = 6$ . There is still a large uncertainty from the choice of the fit ansatz. To remove this, further simulations at lighter quark masses are necessary.

Next, we compare these results with those of a staggered quark action. We plot the results of the pseudo-critical temperature ( $T_{pc}$ ) in unit of Sommer scale ( $r_0$ ) as a function of  $m_{PS} r_0$  in Fig. 2 (right) together with those by the RBC-Bielefeld Collaboration using 2+1 flavor p4-improved staggered quark action.<sup>15)</sup> As seen in this figure, results of  $T_{pc}$  obtained by different quark actions seem to approach the same function of  $m_{PS} r_0$  as  $N_t$  increases.

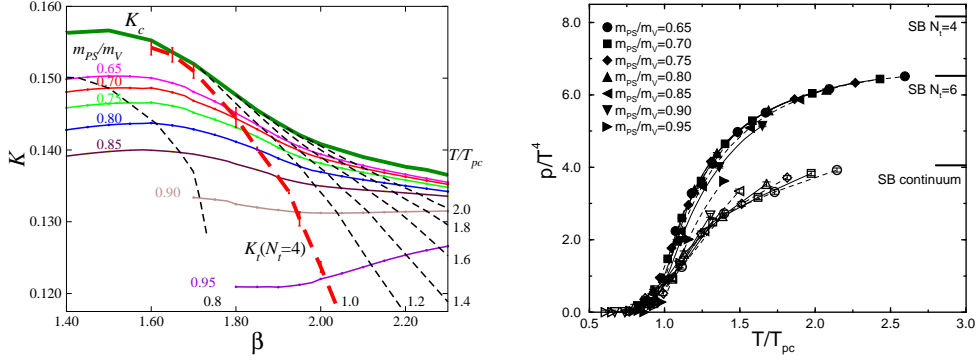


Fig. 3. Left: Lines of constant  $m_{PS}/m_V$  (solid line) and  $T/T_{pc}$  (dashed line) on an  $N_t = 4$  lattice. Right: Pressure as a function of  $T/T_{pc}$  on an  $N_t = 4$  (filled) and 6 (open) for each  $m_{PS}/m_V$ .<sup>2)</sup>

### §5. Equation of state at $\mu_q = 0$ and $\mu_q \neq 0$

The studies of the equation of state (EoS) can provide basic input for the analysis of the experimental signatures for QGP formation, e.g. the EoS will control the properties of any hydrodynamic expansion.

For the study at zero chemical potential, the integral method is commonly used. This method is based on the equation for pressure,  $p = (T/V)\ln Z$ , where  $Z$  is the partition function. Because the derivatives of the partition function can be expressed by expectation values of operators, which are computable by a Monte-Carlo simulation, we obtain the pressure by integrating this expectation value in the parameter space. For the case of the Wilson quark, we have

$$\frac{p}{T^4} = -N_t^4 \int^{(\beta, K)} d\xi \left\{ \frac{1}{N_s^3 N_t} \left\langle \frac{\partial S}{\partial \xi} \right\rangle - (\text{value at } T = 0) \right\} \quad (5.1)$$

with  $d\xi = (d\beta', dK')$  on the integration path. The starting point of the integration path should be chosen such that  $p \approx 0$  there.

The CP-PACS Collaboration carried out a systematic calculation of EOS with a 2 flavor Wilson-type quark action at  $\mu_q = 0$ . They used the RG gauge and the clover quark actions with  $16^3 \times 4$  and  $16^3 \times 6$  lattices.<sup>2)</sup> The translation from the results obtained by Eq. (5.1) as functions of  $(\beta, K)$  to those of physical parameters can be done using Fig. 3 (left). The thin solid lines shows the lines of constant physics (LCP), which they determine by  $m_{PS}/m_V$  (the ratio of pseudo-scalar and vector meson masses at  $T = 0$ ). The chiral limit  $K_c$  corresponds to LCP for  $m_{PS}/m_V = 0$ . The bold dashed line denoted as  $K_t(N_t = 4)$  represents the pseudo-critical line  $T/T_{pc} = 1$  at  $N_t = 4$ . The thin dashed lines represent the lines of constant  $T/T_{pc}$  estimated by  $T/m_V = (N_t m_V a)^{-1}$ .

The right panel of Fig. 3 is the result of the pressure as a function of temperature for each LCP. Filled and open symbols are the results for  $N_t = 4$  and 6 respectively. Different shapes of the symbol correspond to different values of  $m_{PS}/m_V$ , i.e. different quark masses. This figure shows that the pressure is almost independent of the quark mass in a wide range of  $m_{PS}/m_V$ . However, the  $N_t$ -dependence is sizeable,

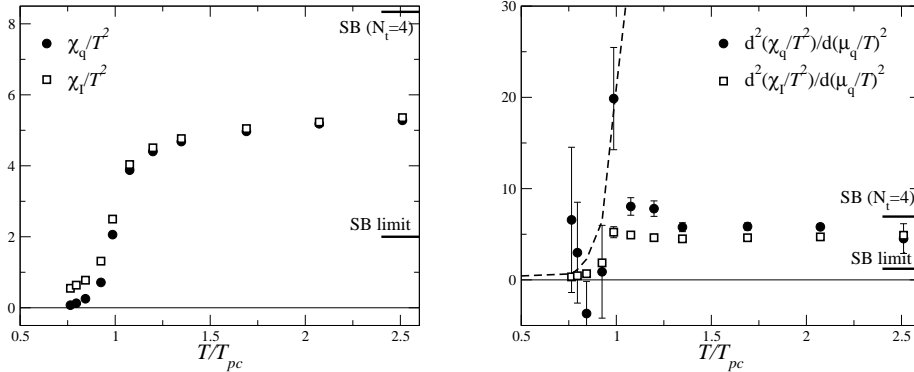


Fig. 4. Left: Quark number (circle) and isospin (square) susceptibilities at  $\mu_q = \mu_I = 0$ . Right: The second derivatives of these susceptibilities.

hence further simulations with large  $N_t$  are important.

On the other hand, the studies of the EoS at non-zero baryon number density is attracting interest widely since the chemical potential dependence of the EoS should explain the difference of experimental results obtained at different beam energy. Moreover, hadronic fluctuations at finite densities are closely related to the appearance of the critical point in the  $(T, \mu_q)$  plane and may be experimentally testable by an event-by-event analysis of heavy ion collisions. The fluctuations can also be studied by numerical simulations of lattice QCD calculating the quark number and isospin susceptibilities,  $\chi_q$  and  $\chi_I$ . They correspond to the second derivatives of the pressure with respect to  $\mu_q$  and  $\mu_I$ , where  $\mu_I$  is the isospin chemical potential. From a phenomenological argument in the sigma model,  $\chi_q$  is singular at the critical point, whereas  $\chi_I$  shows no singularity there.

To investigate the EoS at finite density, the Bielefeld-Swansea Collaboration proposed a Taylor expansion method.<sup>17)</sup> Since Monte-Carlo simulations cannot be performed at finite density due to the sign problem, one evaluates the  $\mu_q$  dependence of  $\ln Z$  by computing the higher order derivatives of  $\ln Z$  instead of integrating the first derivative.

The WHOT-QCD Collaboration performed simulations at  $m_{PS}/m_V = 0.65$  and  $0.80$  on a  $16^3 \times 4$  lattice with the improved Wilson quark action. They calculated the second and fourth derivatives of pressure which correspond to the  $\chi_q$  and  $\chi_I$  and their second derivatives with respect to  $\mu_q$  and  $\mu_I$  at  $\mu_q = \mu_I = 0$ . (Note that the odd derivatives are zero at  $\mu_q = 0$ .)

The left panel of Fig. 4 shows  $\chi_q/T^2$  (circle) and  $\chi_I/T^2$  (square) at  $m_{PS}/m_V = 0.8$  and  $\mu_q = \mu_I = 0$  as functions of  $T/T_{pc}$ . It is found that  $\chi_q/T^2$  and  $\chi_I/T^2$  increase sharply at  $T_{pc}$ , in accordance with the expectation that the fluctuations in the QGP phase are much larger than those in the hadron phase. Their second derivatives  $\partial^2(\chi_q/T^2)/\partial(\mu_q/T)^2$  and  $\partial^2(\chi_I/T^2)/\partial(\mu_q/T)^2$  are shown in Fig. 4 (right). The basic features are quite similar to those found previously with the p4-improved staggered fermions.<sup>17)</sup>  $\partial^2(\chi_I/T^2)/\partial(\mu_q/T)^2$  remains small around  $T_{pc}$ , suggesting that there are no singularities in  $\chi_I$  at non-zero density. On the other hand, we expect a large enhancement in the quark number fluctuations near  $T_{pc}$  as approaching the critical

point in the  $(T, \mu_q)$  plane. The dashed line in Fig. 4 (right) is a prediction from the hadron resonance gas model at low temperature,  $\partial^2 \chi_q / \partial \mu_q^2 \approx 9 \chi_q / T^2$ . Although current statistical errors in Fig. 4 (right) are still large,  $\partial^2(\chi_q/T^2)/\partial(\mu_q/T)^2$  near  $T_{pc}$  is much larger than that at high temperatures. At the right end of the figure, values of free quark-gluon gas (Stefan-Boltzmann gas) for  $N_t = 4$  and for  $N_t = \infty$  limit are shown. Since the lattice discretization error in the EoS is known to be large at  $N_t = 4$  with their quark action, it is needed to extend this study to larger  $N_t$  for the continuum extrapolation.

### §6. Heavy quark free energies

Finally, we discuss a free energy between static quarks. Clarification of the interaction between heavy quarks in QGP is important to understand the properties of charmoniums in heavy ion collisions. The heavy quark free energy  $F_M$  in various color channels  $M$  can be measured separately on the lattice by the correlations of the Polyakov loop with an appropriate gauge fixing.

Recently, the heavy quark free energy for 2 flavor QCD with dynamical Wilson quarks in the Coulomb gauge are studied by the WHOT-QCD Collaboration, using the same configuration for the calculation of the EoS in the previous section.<sup>5)</sup> With the improved actions they adopted, the rotational symmetry is well restored in the heavy quark free energies,<sup>18)</sup> hence it is not necessary to introduce terms correcting lattice artifacts at short distances to analyze the data.

They found that, at  $T > T_{pc}$ , the free energies of  $QQ$  and  $Q\bar{Q}$  normalized to be zero at large separation show attraction (repulsion) in the color singlet and anti-triplet channels (color octet and sextet channels), and fitted the free energy data in each channel by the screened Coulomb form,

$$F_M(r, T) - F_M(\infty, T) = C(M) \frac{\alpha_{\text{eff}}(T)}{r} e^{-m_D(T)r}, \quad (6.1)$$

where  $\alpha_{\text{eff}}(T)$  and  $m_D(T)$  are the effective running coupling and Debye screening mass, respectively. The Casimir factor  $C(M) \equiv \langle \sum_{a=1}^8 t_1^a \cdot t_2^a \rangle_M$  for color channel  $M$  is explicitly given by  $C(\mathbf{1}) = -\frac{4}{3}$ ,  $C(\mathbf{8}) = \frac{1}{6}$ ,  $C(\mathbf{6}) = \frac{1}{3}$ ,  $C(\mathbf{3}^*) = -\frac{2}{3}$ . The results of  $\alpha_{\text{eff}}(T)$  and  $m_D(T)$  are shown in Fig. 5 for  $m_{\text{PS}}/m_V = 0.65$ . They found that there is no significant channel dependence in  $\alpha_{\text{eff}}(T)$  and  $m_D(T)$  at sufficiently high temperatures ( $T \gtrsim 2T_{pc}$ ). In other words, the channel dependence in the free energy can be well absorbed in the kinematical Casimir factor at high temperatures,

The magnitude and the  $T$ -dependence of  $m_D(T)$  is consistent with the next-to-leading order calculation in thermal perturbation theory. Moreover it is also well approximated by the leading order form with an ‘‘effective’’ running coupling defined from  $\alpha_{\text{eff}}(T)$ . On the other hand, by comparing these results with the results by an improved staggered quark action,<sup>19)</sup> they found that  $\alpha_{\text{eff}}(T)$  does not show appreciable difference while  $m_D(T)$  in the Wilson quark action is larger than that of the staggered quark action by 20%. To draw a definite conclusion, however, simulations with smaller lattice spacings, i.e., larger lattice sizes in the temporal direction (such as  $N_t = 6$  or larger) at smaller quark masses are required.

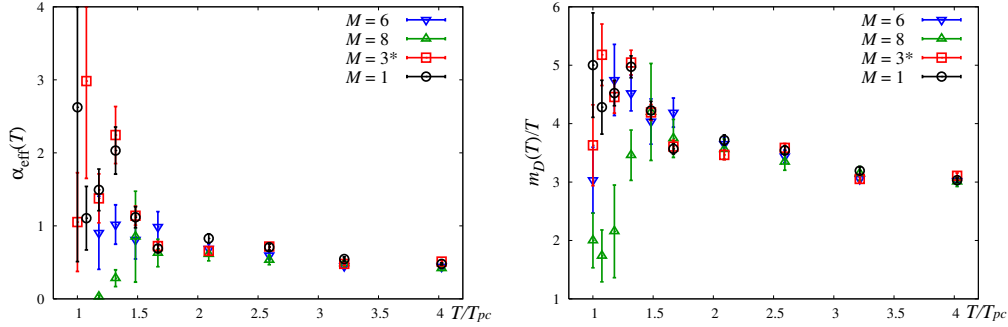


Fig. 5. The effective running coupling  $\alpha_{\text{eff}}(T)$  (left) and Debye screening mass  $m_D(T)$  (right) for each color channel as a function of temperature at  $m_{\text{PS}}/m_{\text{V}} = 0.65$ .

## §7. Summary

We reported the current status of the study of QCD thermodynamics using a Wilson quark action. The basic properties of QCD with 2 flavors of Wilson quarks such as the phase structure and the scaling behavior have been already studied. Moreover, the qualitative agreements between the results obtained by a Wilson quark action and a staggered quark action have been discussed for some thermodynamic quantities. The quantitative improvements are important in the future studies.

I would like to thank the members of the WHOT-QCD Collaboration for collaboration, discussions and comments. This work is supported by Grants-in-Aid of the Japanese MEXT (No. 18740134) and Sumitomo Foundation (No. 050408).

## References

- 1) A. Ali Khan et al. (CP-PACS Collaboration), Phys. Rev. D **63** (2000), 034502.
- 2) A. Ali Khan et al. (CP-PACS Collaboration), Phys. Rev. D **64** (2001), 074510.
- 3) S. Ejiri et al., PoS **LAT2006** (2006), 132.
- 4) Y. Maezawa et al. (WHOT-QCD Collaboration), hep-lat/07020005.
- 5) Y. Maezawa et al. (WHOT-QCD Collaboration), Phys. Rev. D **75** (2007), 074501.
- 6) S. Aoki, Phys. Rev. D **30** (1984), 2653; Phys. Rev. Lett. **57** (1986), 3136; Nucl. Phys. B **314** (1989), 79; S. Aoki, A. Ukawa, and T. Umemura, Phys. Rev. Lett. **76** (1996), 873.
- 7) F. Karsch, Phys. Rev. D **49** (1994), 3791; F. Karsch and E. Laermann, Phys. Rev. D **50** (1994), 6954.
- 8) S. Aoki et al., Phys. Rev. D **57** (1998), 3910.
- 9) E. Laermann, Nucl. Phys. B (Proc. Suppl.) **60A** (1998), 180.
- 10) C. Bernard et al., Phys. Rev. D **61** (2000), 054503.
- 11) M. D'Elia, A. Di Giacomo and C. Pica, Phys. Rev. D **72** (2005), 114510.
- 12) Y. Iwasaki, K. Kanaya, S. Kaya and T. Yoshie, Phys. Rev. Lett. **78** (1997), 179.
- 13) M. Bochicchio et al., Nucl. Phys. B **262** (1985), 331.
- 14) C. Bernard et al., Phys. Rev. D **71** (2005), 034504.
- 15) M. Cheng et al., Phys. Rev. D **74** (2006), 054507.
- 16) Y. Aoki, Z. Fodor, S.D. Katz and K.K. Szabo, Phys. Lett. B **643** (2006), 46.
- 17) C.R. Allton et al., Phys. Rev. D **66** (2002), 074507; C.R. Allton et al., Phys. Rev. D **68** (2003), 014507; C.R. Allton et al., Phys. Rev. D **71** (2005), 054508.
- 18) S. Aoki et al. (CP-PACS Collaboration), Phys. Rev. D **60** (1999), 114508.
- 19) O. Kaczmarek and F. Zantow, Phys. Rev. D **71** (2005), 114510; M. Döring, et al., Eur. Phys. J. C **46** (2006), 179.